BNL-93905-2010-IR

C-A/AP/#393
August 2010

Dynamic aperture calculation for the RHIC 2010 100 GeV Au-Au run lattices

Y. Luo, K. Brown, W. Fischer, V. Ptitsyn, T. Roser, V. Schoefer, S. Tepikian, D. Trbojevic
Brookhaven National Laboratory, Upton, NY 11973, USA

Collider-Accelerator Department
Brookhaven National Laboratory
Upton, NY 11973

April 1, 2010

Dynamic aperture calculation for the RHIC 2010 100 GeV Au-Au run lattices

Y. Luo, K. Brown, W. Fischer, V. Ptityn, T. Roser, V. Schoefer, S. Tepikian, D. Trbojevic
Brookhaven National Laboratory, Upton, NY 11973, USA

In this note we summarize the dynamic aperture calculation with the 2010 RHIC 100 GeV Au-Au run lattices. This study was initiated to understand the observed large beam decay in the Yellow ring after rf re-bucketing in the beginning of this run. The off-line linear lattice models and the interaction region non-linearity models are used. The large beam decay in the Yellow ring after re-bucketing was eventually eliminated by lowering the Yellow tunes to 0.21 from 0.235 with $\beta^* = 0.7$m lattice. In this note we only focus on the numeric simulation instead of the beam experiments.

1 Introduction

The design β^*s at IP6 and IP8 for the 2010 RHIC 100 GeV Au-Au run were initially 0.6 m. The β^*s at all other non-colliding IPs are 4.0 m. The design working points were (0.23, 0.22). In the operation in the beginning of this run, the tunes were around (0.235, 0.225) for both rings. The difference of this run other than the previous 2007 Au-Au run and 2008 d-Au run is that the intra-beam scattering (IBS) suppression lattice with reduced $\beta^* = 0.6$ m was used. The β^*s were 0.8 m in the 2007 Au-Au run. In 2008 d-Au run, we used the IBS suppression lattice with $\beta^* = 0.8$ m in the Yellow ring. We also demonstrated IBS suppression lattice with $\beta^* = 0.7$ m in the Yellow ring in the beam experiment [1]. With the IBS suppression lattice, the betatron phase advances of arc FODO cell are increased to around 90°.

As we know, low β^* will increase the strengths of chromatic sextupoles to correct the increased natural linear chromaticity. The second order chromaticities will increase too. And in the interaction regions, the particles with large transverse amplitude and large off-momentum deviation will sample more non-linearities and therefore the off-momentum dynamic aperture will be reduced. The maximum dispersion in the IR6 and IR8 is about m for the $\beta^* = 0.6$ m lattice.

To shorten the bunch length, rf re-bucketing is used in RHIC ion runs. The difference is that this year the total rf voltage with rf re-bucketing is 4.5 MV, 1.0 MV more than that in the previous 2007 and 2008 ion runs. RF re-bucketing reduces the full width bunch length from 20 ns seconds to 5 ns seconds but it increases the momentum spread from 1.1×10^{-3} to 1.7×10^{-3} [2].

To save the training time of DX magnets, there are 2.0 mrad beam-to-beam crossing angles at non-colliding interaction points (IPs) for this run.

In the following, we will first calculate the off-momentum tunes and the off-momentum beta-beat with $\beta^* = 0.6$ m lattices. Then we calculate the dynamic apertures in a tune scan with $\beta^* = 0.6$ m and $\beta^* = 0.7$ m. The effect of second order chromaticity correction on the dynamic aperture is checked with $\beta^* = 0.7$ m lattice. Dynamic apertures with relaxed β^* are also calculated.

2 Off-momentum tunes and β-beat for $\beta^* = 0.6$m lattices

For the lattices with $\beta^* = 0.6$ m, Figure 1 shows the off-momentum tunes. The left plot shows the horizontal off-momentum tunes and the right one shows the off-momentum vertical tunes. The on-momentum tunes are set to (31.23, 32.22). As a comparison, we also shows the off-momentum tunes of the RHIC 2008 Yellow ring lattice with $\beta^* = 1.0$ m.

From Figure 1, when the off-momentum deviation $dp/p_0 = 1.7 \times 10^{-3}$, the horizontal tune in the Blue ring crosses 31.2 (5th order betatron resonance) and the horizontal tune in Yellow ring crosses 31.25 (4th order betatron resonance). With $dp/p_0 = -1.7 \times 10^{-3}$, the Blue vertical tune goes down to 0.208. With $dp/p_0 = 1.7 \times 10^{-3}$, the Yellow vertical tune goes up to 0.233.

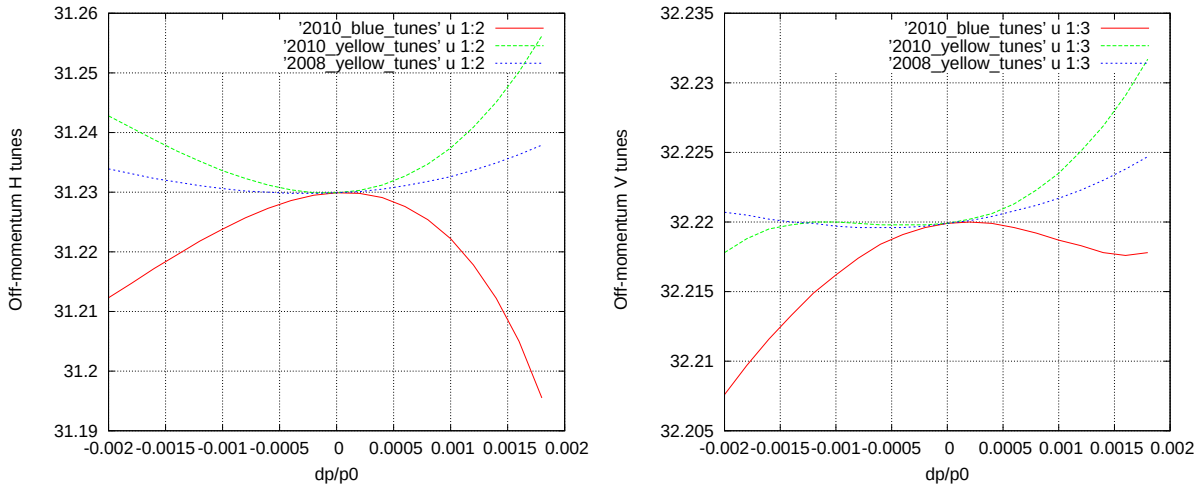

Figure 1: Left: Horizontal off-momentum tunes. Right: Vertical off-momentum tunes

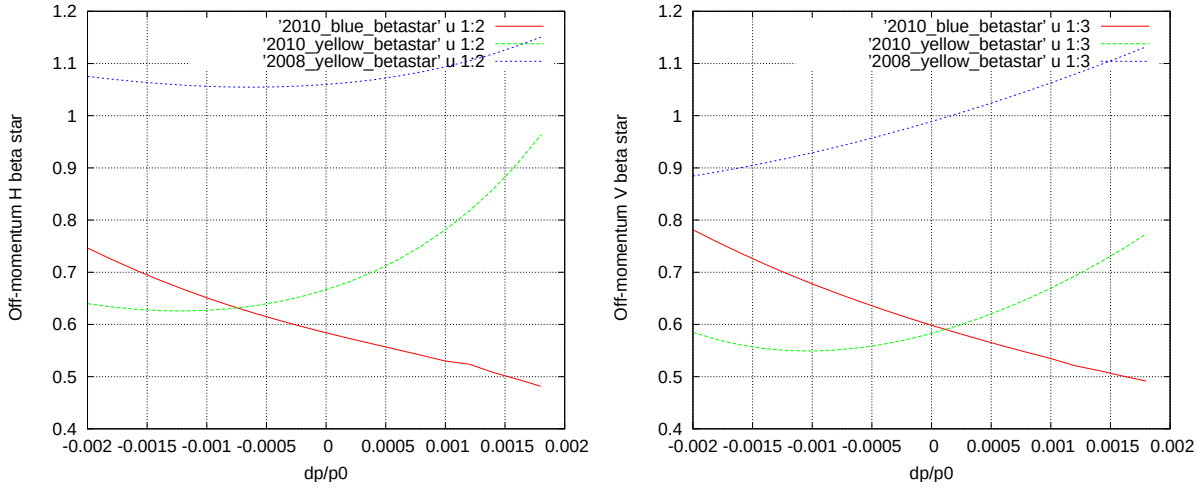

Figure 2: Left: Horizontal off-momentum β^*. Right: Vertical off-momentum β^*.

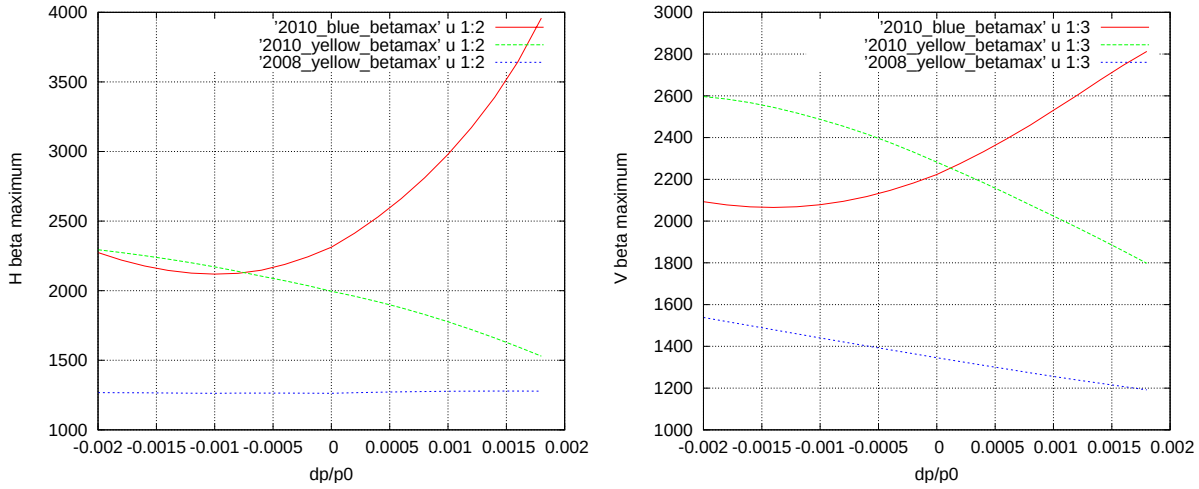

Figure 3: Left: Horizontal off-momentum β_{max}. Right: Vertical off-momentum β_{max}.

As we mentioned earlier, the maximum momentum deviation reaches $\pm 1.7 \times 10^{-3}$ after rf re-bucketing. Therefore, with the $\beta^* = 0.6$ m lattices, the particles with large dp/p_0 in both rings will have reduced dynamic apertures and tend to be lost after re-bucketing.

Figure 2 shows the off-momentum β^* for both rings. From Figure 2, the horizontal and vertical β^*s in the Blue ring keeps on decreasing when dp/p_0 increases from 0 to 1.7×10^{-3}. The β^*s for $dp/p_0 = 1.7 \times 10^{-3}$ are less than 0.5 m. For the Yellow ring, β^* goes smaller than 0.6 m with negative momentum deviation. As we know, low off-momentum β^* will cause large off-momentum β_{max} in the triplets of the colliding IRs. Figure 3 shows the maximum off-momentum β_{max} for both rings. For example, for the Blue ring, the horizontal β_{max} exceeds 3500 m with $dp/p_0 > 1.5 \times 10^{-3}$.

From Figure 1, for the 2010 $\beta^* = 0.6$ m lattices, the second order chromaticity dominates the off-momentum tunes. The second order chromaticity is define as $\frac{1}{2}\frac{\partial^2 Q_{x,y}}{\partial \delta^2}$. With the off-line lattice models, the second order chromaticities for the Blue ring are (-6673.99, -2595.84). The second order chromaticities for the Yellow ring are (5593.38, 1980.28). However, in the beam experiment we measured less than 2500 in both rings with rf radial shifts up to 0.5 mm which is equavilent to $dp/p_0 = 0.5 \times 10^{-3}$. A radial excursion of at least 0.5 mm is needed for a visible measurement. The reason for the large discrepancy between predictiona dn measurement of second order chromaticity in this run is under investigation.

3 Dynamic aperture with $\beta^* = 0.6$m lattices

Here we calculate the dynamic apertures with $\beta^* = 0.6$ m lattices. The dynamic apertures are searched in 5 phase angles in the first quadrant in the x-y plane. Th dynamic apertures are given in the unit of transverse rms beam sizes σ, $1\sigma = \sqrt{\epsilon_n \beta^*/\gamma}$. ϵ_n is the normalized transverse rms emittance. γ is the relativistic factor of the ions. In the simulation, the proton-proton beam-beam interactions at IP6 and IP8 are modeled as 4-D transverse kicks although the bunch length is bigger than β^* before the rf re-bucketing.

In our simulation, we assume that the total rf voltage is 400 kV and the rf harmonic number is 360 before rf re-bucketing. With rf re-bucketing, the total rf voltage is set to 4 MV and the rf harmonic number is 2520. Rf re-bucketing shortens the bunch full width length from 20 μs to 5 μs. That is, one rms bunch length is reduced from 1.0 m to 0.25 m. However, rf re-bucketing increases the bunch momentum spread from $\pm 1.1 \times 10^{-3}$ to $\pm 1.7 \times 10^{-3}$.

Table 1 shows the calculated dynamic apertures with and without rf re-bucketing. For each case we calculate the dynamic aperture with several off-momentum deviations. From Table 2, with $\beta^* = 0.6$ m, for particles with $dp/p_0 = \pm 0.9 \times 10^{-3}$, the minimum dynamic apertures are above 3.2σ in the Blue ring and 4.0 σ in the Yellow ring. With rf re-bucketing, for $dp/p_0 = \pm 1.7 \times 10^{-3}$, the minimum dynamic apertures drop to 1.0 σ in the Blue ring and 2.4 σ in the Yellow ring. Therefore, after rf re-bucketing, the particles with large off-momentum deviations in the bunch tend to be lost.

Table 1 also shows that there is more dynamic aperture reduction for off-momentum particles in the Blue ring than that in the Yellow. This agrees with the above calculation of off-momentum tunes, β^*, and β_{max}. However, in the operation, we observed more beam loss in the Yellow ring than in the Blue ring after rf re-bucketing.

4 Tune scan with $\beta^* = 0.6$m lattices

To increase the off-momentum dynamic aperture, we corrected the second order chromaticities in operation. However, we still observed large beam loss in the chromaticity measurement even with second order chromaticities corrected below 500 in the Yellow ring.

As we mentioned earlier, with rf re-bucketing, the momentum tune spread will will increase from $\pm 1.1 \times 10^{-3}$ to $\pm 1.7 \times 10^{-3}$. Another thought for the large Yellow beam decay after rf re-bucketing is that the working point (0.235, 0.225) may be too close to the forth order resonance. In the beam transfer function (BTF) measurements, we observed spurious peaks in the horizontal Yellow spectrum.

In the following, still with the $\beta^* = 0.6$ m lattices, we scan the working points along the diagonal line in the tune space from 0.2 to 1/3. The tunes are adjusted with the focusing and defocusing quadrupoles in the FODO cells in the arc. In this simulation, the rf re-bucketing is on.

Figure 4 shows the dynamic apertures for particles with $dp/p_0 = 0.6 \times 10^{-3}$ in the tune scan from 0.2 to 1/3. From Figure 4, for particles with $dp/p_0 = 0.6 \times 10^{-3}$, there are two dips in the dynamic apertures around resonance lines at 0.25 and 1/3. For the Yellow ring, the dynamic aperture is a little bit larger in the range of (0.2, 0.25) than that in the range of (0.25, 1/3) although the tune space is wider in the tune

Table 1: Calculated 10^6 turn dynamic aperture with $\beta^* = 0.6$ m lattices

	Re-bucketing	dp/p_0	Dynamic aperture [unit: σ]					
			15°	30°	45°	60°	75°	Minimum
Blue ring:								
	No	-0.0009	4.0	3.8	3.8	3.8	4.0	3.8
	No	-0.00045	4.5	4.1	4.1	3.8	4.0	3.8
	No	0.000	4.7	4.5	4.7	5.3	4.7	4.5
	No	0.00045	4.1	4.1	4.0	3.8	4.0	3.8
	No	0.0009	3.2	3.2	3.4	3.6	3.8	3.2
	Yes	-0.0017	1.4	1.6	1.4	1.4	1.6	1.4
	Yes	-0.0009	4.0	3.6	4.0	3.8	3.8	3.6
	Yes	0.000	4.7	4.5	4.7	5.3	4.7	4.5
	Yes	0.0009	3.6	3.4	3.4	3.4	3.4	3.4
	Yes	0.00017	1.0	1.0	1.0	1.2	1.2	1.0
Yellow ring:								
	No	-0.0009	4.7	4.1	4.1	4.1	4.5	4.1
	No	-0.00045	5.1	4.3	4.0	4.1	4.5	4.0
	No	0.000	5.5	5.1	4.9	5.1	5.3	4.9
	No	0.00045	5.3	4.5	4.5	4.5	4.9	4.5
	No	0.0009,	5.1	4.7	4.5	4.7	4.9	4.5
	Yes	-0.0017	3.0	2.8	2.4	2.6	3.2	2.4
	Yes	-0.0009	4.3	4.3	4.0	4.0	4.0	4.0
	Yes	0.000	5.7	5.3	4.9	5.3	5.1	4.9
	Yes	0.0009	5.1	4.7	4.5	4.3	4.5	4.3
	Yes	0.0017	4.0	3.6	3.4	3.2	3.8	3.2

range of (0.25, 1/3). For the Blue ring, the dynamic apertures are comparable in those two tune ranges. In Figure 4, The dynamic aperture dips at some tunes and that can be explained with high order resonances.

Figure 5 shows the dynamic apertures for particles with $dp/p_0 = 1.7 \times 10^{-3}$ in the tune scan from 0.1 to 1/3. The design tune for the ion run was around 0.17 0.19 in the RHIC design phase. From Figure 5, the dynamic aperture is much bigger in the Yellow ring than in the Blue ring.

For the Blue ring, the dynamic aperture is much smaller than that with $dp/p_0 = 0.6 \times 10^{-3}$ shown in Figure 4. There is no dynamic aperture for particles with $dp/p_0 = 1.7 \times 10^{-3}$ below tune 0.15. For the Yellow ring, with $dp/p_0 = 1.7 \times 10^{-3}$, the plateau of dynamic aperture happens between 0.2 and 0.225. Below 0.2, there are several up-down structures in the dynamic apertures. This may be caused by high order resonances.

5 Dynamic apertures with relaxed β^* lattices

Since second order chromaticity correction didn't improve the lifetime in the Yellow ring during rf re-bucketing, we released the design β^* to 0.7 m. $\beta^* = 0.7$ m lattice was demonstrated in the Yellow ring in the beam experiment in the 2008 RHIC 100 GeV d-Au run, although at that time the rf re-bucketing voltage was less than 4 MV. Table 4 lists the exact calculated β^* from the off-line lattice models with different β^*s. Actual β^* in the real machine may vary.

First we calculate and compare the dynamic apertures of the Yellow ring with different β^*s. Off-momentum deviation $dp/p_0 = 1.7 \times 10^{-3}$ is used. The second order chromaticity correction was not applied in the study. With the $\beta^* = 0.7$ m lattices, the calculated second order chromaticities are (-4943.36, -1014.32) in the Blue ring and are (3735.61, 1675.94) in the Yellow ring.

Table 3 shows the dynamic apertures with different values of β^*s in the 10^5 and 10^6 turn trackings. 10^5 turn tracking was performed to provide a quick estimate which β^* we would relax to obtain decent dynamic aperture with rf re-bucketing. Figure 6 shows the dynamic apertures in 5 angles in the x-y plane in the 10^6 turn tracking. From Table 3, either in the 10^5 turn tracking or in the 10^6 turn tracking, there is a large dynamic aperture increase from $\beta^* = 0.6$ m and $\beta^* = 0.7$ m lattices to $\beta^* = 0.8$ m lattice.

With $\beta^* = 0.7$ m lattices, experimentally we were able to measure off-momentum tunes with rf radial shift

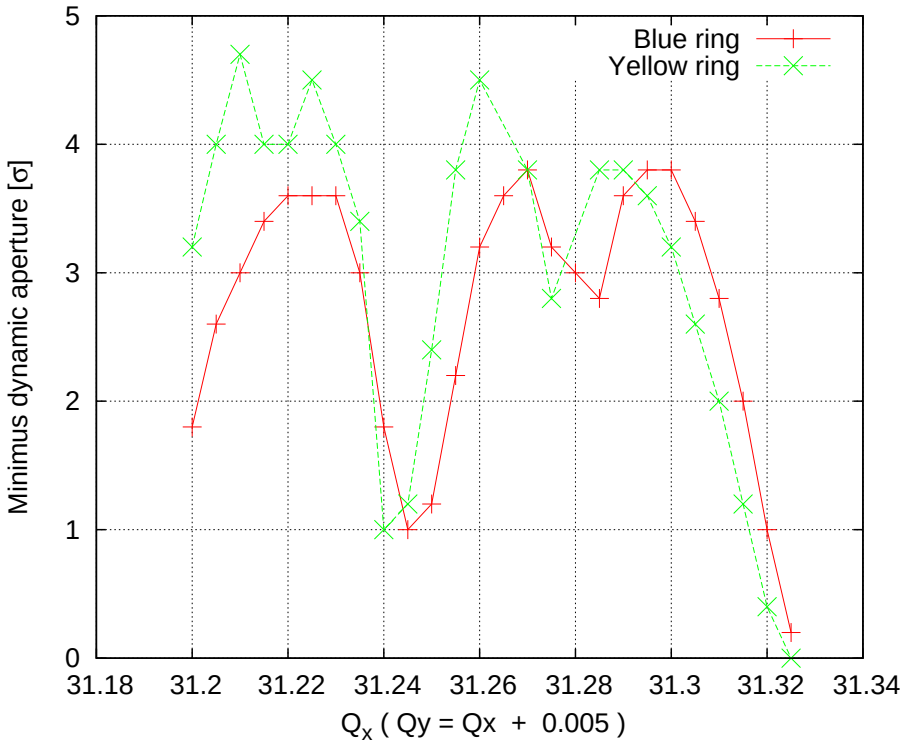

Figure 4: Calculated 10^6 turn dynamic apertures in the tune scan between from 0.2 to 1/3. $\beta^* = 0.6$ m lattices are used. Relative off-momentum deviation $dp/p_0 = 0.6 \times 10^{-3}$. RF re-bucketing is on (Vrf = 4 MV, h = 2520).

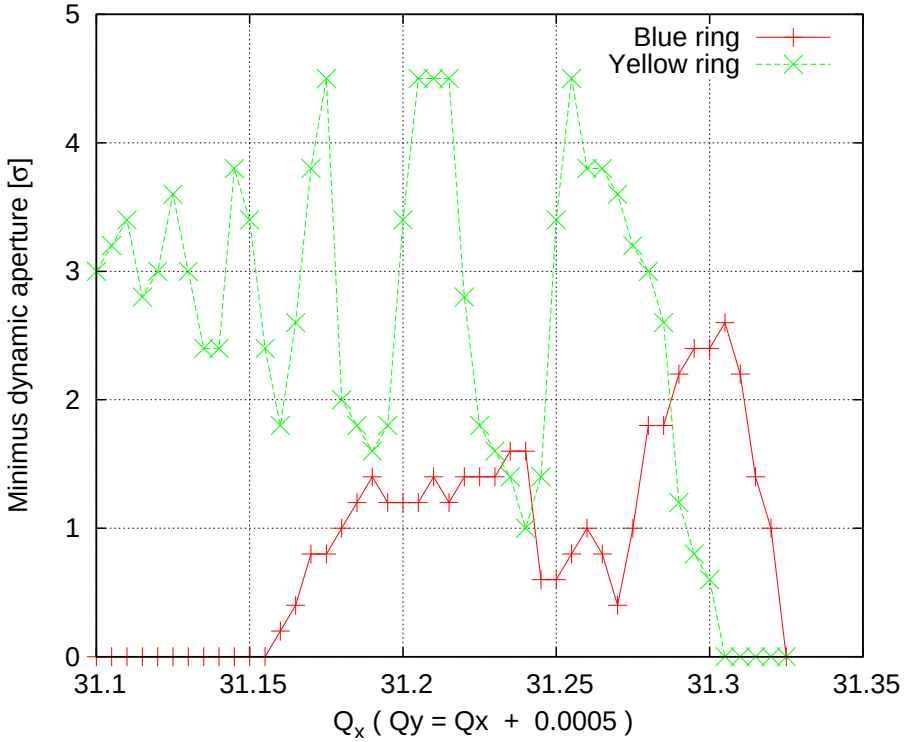

Figure 5: Calculated 10^6 turn dynamic apertures in the tune scan from 0.1 to 1/3. $\beta^* = 0.6$ m lattices are used. Relative off-momentum deviation $dp/p_0 = 1.7 \times 10^{-3}$. RF re-bucketing is on (Vrf = 4 MV, h = 2520).

Table 2: β^*s at IP6 in the Yellow ring for the relaxed β^* lattices

lattice	β_x^* [m]	β_y^* [m]
0.6 m lattice	0.65	0.56
0.7 m lattice	0.76	0.66
0.8 m lattice	0.86	0.76
0.9 m lattice	0.98	0.85
1.0 m lattice	1.1	0.95

Table 3: Calculated Yellow ring dynamic aperture with $\beta^* = 0.6$ m lattices

β^*	Dynamic aperture [unit: σ]					
	15°	30°	45°	60°	75°	Minimum
10^5 **turns:**						
0.6	2.6	2.8	2.4	2.2	4.2	2.6
0.7	3.2	3.8	3.8	5.8	6.0	3.2
0.8	5.0	5.2	6.3	6.3	6.5	5.0
0.9	5.3	6.3	6.9	7.1	7.2	5.3
1.0	6.2	7.1	7.5	7.9	7.9	6.2
10^6 **turns:**						
0.6	2.4	2.1	2.2	2.2	4.0	2.1
0.7	3.0	3.4	3.0	5.2	5.6	3.0
0.8	4.8	4.8	5.8	5.8	6.2	4.8
0.9	5.2	5.8	6.5	6.3	7.1	5.2
1.0	6.0	6.3	6.9	7.1	7.7	6.0

up to 0.8 mm which corresponds to $dp/p - 0 = 0.9 \times 10^{-3}$. The measured second order chromaticities were about (-300, -1500) in the Blue ring and about (2000, 1200) in the Yellow ring. However, with $\beta^* = 0.7$ m lattice, operationally we still observe more than 100%/hour beam decay in the Yellow ring after rf re-bucketing.

6 Tune scan with $\beta^* = 0.7$ m lattices

In this section we perform tune scan with the $\beta^* = 0.7$ m lattices. As comparison, we calculate the dynamic apertures without and with second order chromaticities. The second order chromaticities are roughly corrected below 100 with 4 knob method. In the following simulation, we only calculate the dynamic apertures for particles with $dp/p_0 = 1.7 \times 10^{-3}$.

Figure 6 shows the dynamic apertures without second order chromaticity correction. Comparing Figure 6 with Figure 5, $\beta^* = 0.7$ m lattice gives larger dynamic apertures for particles with $dp/p_0 = 1.7 \times 10^{-3}$ than that with $\beta^* = 0.6$ m. The dynamic apertures in the Blue ring are still far less than that in the Yellow ring.

To understand why the Yellow ring has much larger dynamic aperture than Blue ring, we re-do the above tune scan without IR nonlinear field errors. IR nonliear field errors play an crucial role in the dynamic aperture reduction in the RHIC rings. Figure 7 shows the minimum dynamic apertures in this scan . From Figure 7, the dynamic apertures in the both rings increase without IR nonlinearities. However, we still observe the large difference in the maximum dynamic aperures between the Blue and Yellow ring.

Figure 8 shows the dynamic apertures with second order chromaticity correction. The IR nonlinearities are included in this study. With second order chromaticity correction, the dynamic apertures for particles with $dp/p_0 = 1.7 \times 10^{-3}$ in the Blue ring increased to about 4σs and are comparable with that in the Yellow ring.

The large difference in the calculated maximum dynamic apertures between the Blue and Yellow rings may be explained by the second order chromaticities. As we mentioned earlier, for the $\beta^* = 0.7$ m lattices, the calculated second order chromaticities from the lattice model are (-4943.36, -1014.32) in the Blue ring and are (3735.61, 1675.94) in the Yellow ring. However, in the operation, we measured second order chromaticities about (-300, -1500) in the Blue ring and about (2000, 1200) in the Yellow ring.

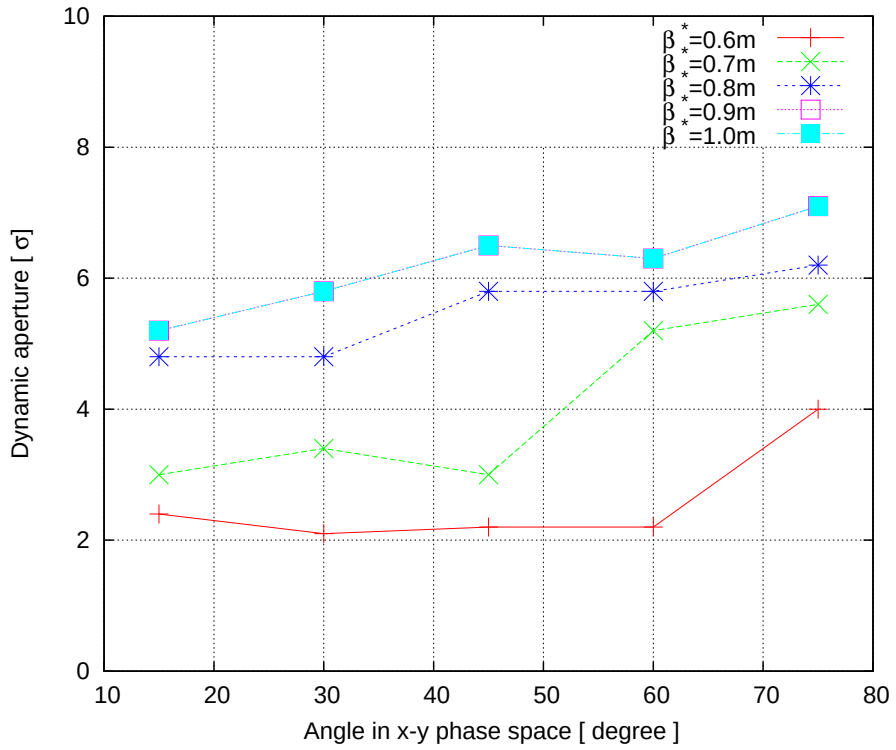

Figure 6: 10^6 turn Yellow ring dynamic apertures with different β^* at IP6 and IP8. Relative off-momentum deviation dp/p_0=0.0017. RF re-bucketing is on (Vrf = 4 MV, h = 2520).

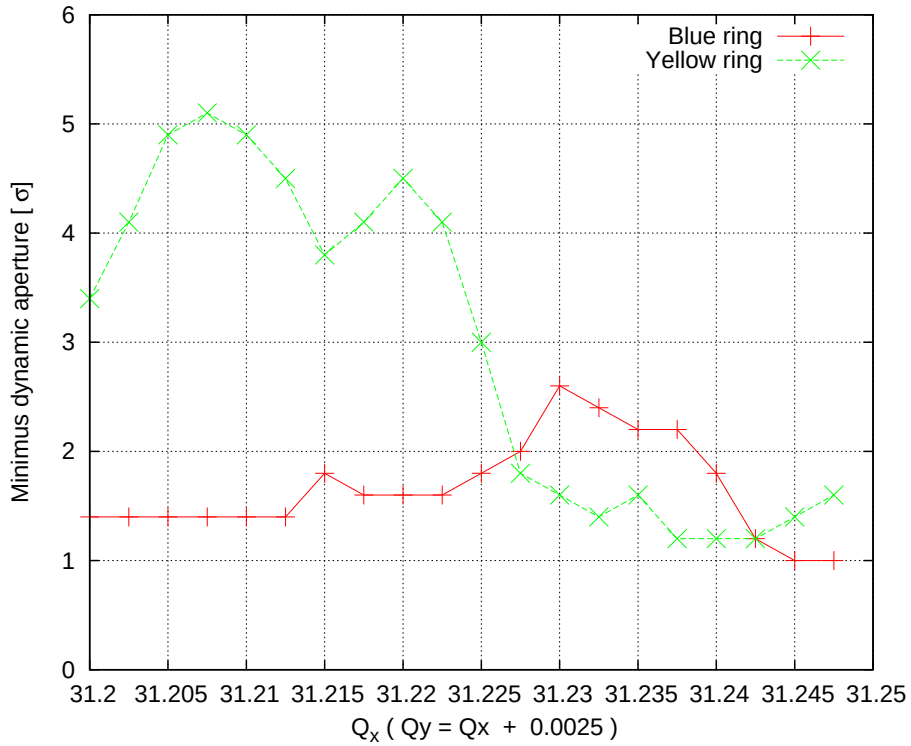

Figure 7: 10^6 turn dynamic apertures without second order chromaticity correction in the tune scan from 0.2 to 0.25. β^* = 0.7 m lattices used. Relative off-momentum deviation dp/p_0=0.0017. RF re-bucketing is on (Vrf=4MV, h=2520).

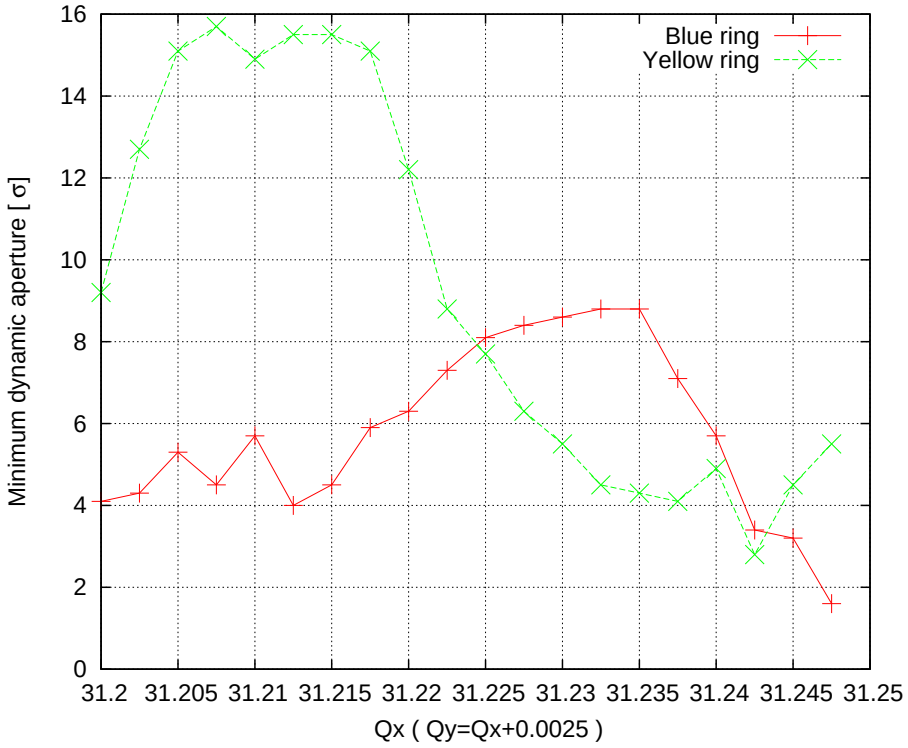

Figure 8: 10^6 turn dynamic apertures without IR multipole field errors and without second order chromaticity correction in the tune scan from 0.2 to 0.25. $\beta^* = 0.7$ m lattices used. Relative off-momentum deviation $dp/p_0 = 0.0017$. RF re-bucketing is on (Vrf=4MV, h=2520).

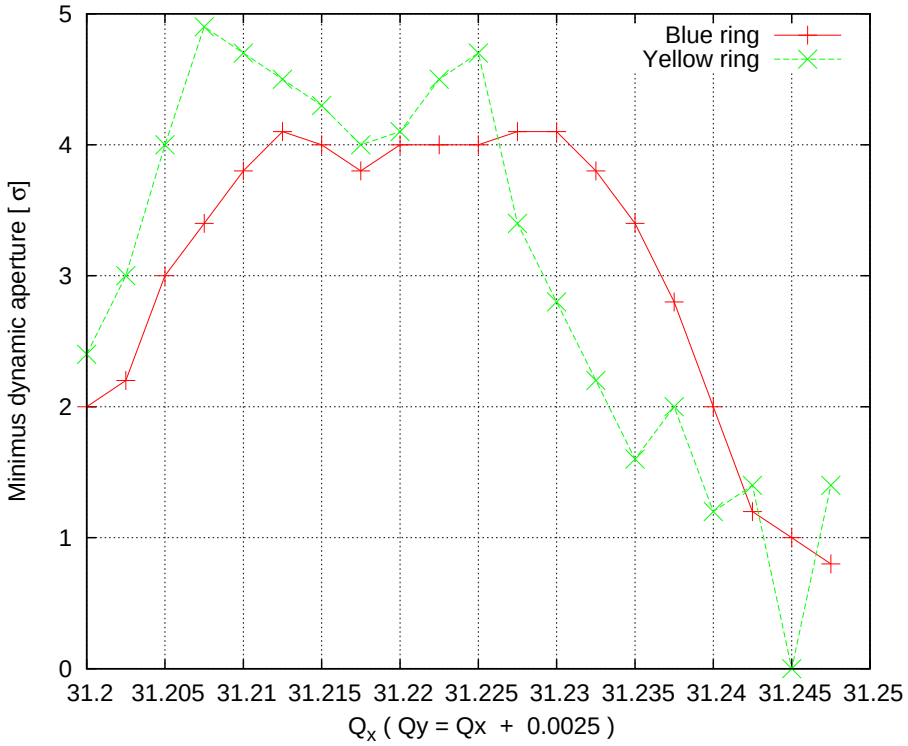

Figure 9: 10^6 turn dynamic apertures with second order chromaticity correction in the tune scan from 0.2 to 0.25. $\beta^* = 0.7$ m lattices used. Relative off-momentum deviation $dp/p_0 = 0.0017$. RF re-bucketing is on (Vrf=4MV, h=2520).

From Figure 6 and Figure 8, for particles with $dp/p_0 = 1.7 \times 10^{-3}$, the maximum dynamic aperture plateau happens in the range of (0.205, 0.225) in the Yellow ring and in the range of (0.215, 0.235) in the Blue ring. In the beam experiment, we scanned the Yellow tunes down to around 0.21 along the diagonal and we were able to measure off-momentum tunes with rf radial shift up to 1.5 mm which corresponds to $dp/p_0 = 1.4 \times 10^{-3}$. Later on the beam decay was eventually reduced below 50%/hour in the Yellow ring during rf re-bucketing with the tune settings (0.21, 0.205). The blue ring tunes are not chnaged. The beam decay in the Blue ring during rf re-bucketing is comparable to that in the Yellow with new working point.

7 Summary

In this note we systematically calculated the dynamic apertures with the 2010 RHIC 100 GeV Au-Au run lattices. We scan the tunes with the $\beta^* = 0.6$ m and $\beta^* = 0.7$ m lattices for both rings. We also checked the effects of the second order chromaticity correction with $\beta^* = 0.7$ m lattice. The dynamic apertures with enlarged β^*s were calculated too. The large beam decay in the Yellow ring after re-bucketing was eventually eliminated by lowering the Yellow tunes to 0.21 from 0.235 with $\beta^* = 0.7$m lattice.

In the simulation, we noticed that the discrepancies between the predictions and the real machine observations. For example, the predicted second order chromaticities are around 5000 with $\beta^* = 0.6$m lattices, while the measured ones were below 2000. And simulation predicts that the Blue ring should have less dynamic aperture than that in the Yellow ring, while in the operation Yellow ring suffered more beam loss than that in Blue ring during the rf re-bucketing. Therefore, our off-line lattices models and IR non-linearity models [5] need further improvements.

There were many people in C-AD who were actively involved in the campaign to understand and to increase the Yellow lifetime during the rf re-bucketing. We apologize that we couldn't inlcude all of their names in this short simulation note although their effects are highly appreciated.

All the simulations in the Note were done with SimTrack [6]. SimTrack is a c++ library for optical calculation and particle tracking in high energy circular accelerators.

References

[1] F. Pilat, et al, *Beta* squeesing in the RHIC*, in the Proceedings of PAC'09.

[2] M. Blaskiewicz, private communications.

[3] Y. Luo and D. Trbojevic, RHIC accelerator physics experimental (APEX) reports, Jan. 26-27, 2010.

[4] V. Schoefer, Y. Luo, and D. Trbojevic, RHIC APEX reports, Feb. 3, 2010.

[5] J. Beebe-Wang and A. Jain, *Realistic non-linear model and field quadlity analysis in RHIC Interaction Regions*, in the Proceedings of PAC'07.

[6] Y. Luo, *SimTrack User's Mannual (v1.0)*, BNL C-AD AP Note 388, January, 2010.

8 Appendix:

Table 4: Tune scan with $\beta^* = 0.6$ m lattices. dp/p0=0.0006 and with re-bucketing.

	Workign points	Dynamic aperture [unit: σ]					
		15°	30°	45°	60°	75°	Minimum
Blue ring:							
	31.2 / 32.205	1.8	2.2	2.2	2.4	2.6	1.8
	31.205 / 32.21	2.6	2.6	2.8	3.0	3.6	2.6
	31.21 / 32.215	3.0	3.2	3.2	3.4	3.8	3.0
	31.215 / 32.22	3.6	3.4	3.6	3.6	4.0	3.4
	31.22 / 32.225	4.0	3.8	3.6	3.8	4.1	3.6
	31.225 / 32.23	3.6	4.0	3.8	3.8	4.1	3.6
	31.23 / 32.235	3.8	3.8	3.8	3.6	3.8	3.6
	31.235 / 32.24	3.6	3.4	3.0	3.0	3.0	3.0
	31.24 / 32.245	3.4	3.2	2.2	2.0	1.8	1.8
	31.245 / 32.25	2.4	1.8	1.6	1.2	1.0	1.0
	31.25 / 32.255	1.2	1.4	1.6	1.6	2.4	1.2
	31.255 / 32.26	2.2	2.2	2.4	2.6	3.2	2.2
	31.26 / 32.265	3.2	3.2	3.2	3.4	3.6	3.2
	31.265 / 32.27	3.6	3.6	3.8	3.8	4.0	3.6
	31.27 / 32.275	3.8	4.0	4.0	4.1	3.8	3.8
	31.275 / 32.28	4.0	4.0	4.0	3.4	3.2	3.2
	31.28 / 32.285	3.8	3.4	3.2	3.6	3.0	3.0
	31.285 / 32.29	2.8	2.8	3.2	3.2	4.1	2.8
	31.29 / 32.295	3.6	3.6	3.8	4.1	3.8	3.6
	31.295 / 32.3	3.8	3.8	3.8	3.8	4.0	3.8
	31.3 / 32.305	3.8	4.0	4.0	4.0	4.0	3.8
	31.305 / 32.31	3.8	3.8	3.8	3.8	3.4	3.4
	31.31 / 32.315	3.4	3.0	3.0	3.0	2.8	2.8
	31.315 / 32.32	2.8	2.4	2.2	2.0	2.0	2.0
	31.32 / 32.325	1.6	1.0	1.2	1.2	1.2	1.0
	31.325 / 32.33	0.2	0.2	0.2	0.2	0.2	0.2
Yellow ring:							
	31.2 / 32.205	3.8	3.2	3.8	3.8	4.0	3.2
	31.205 / 32.21	4.0	4.0	4.3	4.1	4.9	4.0
	31.21 / 32.215	4.7	5.1	4.7	4.7	4.7	4.7
	31.215 / 32.22	4.7	4.3	4.9	4.0	4.1	4.0
	31.22 / 32.225	4.1	4.0	4.3	4.7	4.9	4.0
	31.225 / 32.23	4.7	4.7	4.5	4.5	4.7	4.5
	31.23 / 32.235	4.3	4.3	4.1	4.0	4.1	4.0
	31.235 / 32.24	3.8	3.6	3.6	3.4	3.4	3.4
	31.24 / 32.245	2.2	1.8	1.6	1.0	1.0	1.0
	31.245 / 32.25	1.6	1.2	1.2	1.2	1.8	1.2
	31.25 / 32.255	2.4	2.4	2.4	3.4	3.8	2.4
	31.255 / 32.26	3.8	4.0	3.8	4.1	4.1	3.8
	31.26 / 32.265	4.7	4.7	4.7	4.5	4.7	4.5
	31.265 / 32.27	4.4	4.2	4.4	4.6		4.2
	31.27 / 32.275	4.5	4.1	4.0	3.8	4.0	3.8
	31.275 / 32.28	3.2	3.0	2.8	3.0	3.0	2.8
	31.28 / 32.285	3.0	2.6	2.6	2.8		2.6
	31.285 / 32.29	4.0	4.0	3.8	4.1	3.8	3.8
	31.29 / 32.295	4.1	4.0	4.0	4.1	3.8	3.8
	31.295 / 32.3	4.0	3.8	3.6	3.8	3.8	3.6
	31.3 / 32.305	3.4	3.4	3.2	3.2	3.4	3.2
	31.305 / 32.31	2.6	2.6	2.6	2.6	2.6	2.6
	31.31 / 32.315	2.2	2.0	2.0	2.0	2.0	2.0
	31.315 / 32.32	1.4	1.2	1.2	1.2	1.2	1.2
	31.32 / 32.325	0.4	0.4	0.4	0.4	0.4	0.4
	31.325 / 32.33	0.0	0.0	0.0	0.0	0.0	0.0

Table 5: Calcaulated DA in the tune scan of Blue ring with $\beta^* = 0.6$ m lattices. dp/p0=0.0017 and with re-bucketing.

Workign points	Dynamic aperture [unit: σ]					
	15°	30°	45°	60°	75°	Minimum
Blue ring:						
31.1 / 32.105	0.0	0.0	0.0	0.0	0.0	0.0
31.105 / 32.11	0.0	0.0	0.0	0.0	0.0	0.0
31.11 / 32.115	0.0	0.0	0.0	0.0	0.0	0.0
31.115 / 32.12	0.0	0.0	0.0	0.0	0.0	0.0
31.12 / 32.125	0.0	0.0	0.0	0.0	0.0	0.0
31.125 / 32.13	0.0	0.0	0.0	0.0	0.0	0.0
31.13 / 32.135	0.0	0.0	0.0	0.0	0.0	0.0
31.135 / 32.14	0.0	0.0	0.0	0.0	0.0	0.0
31.14 / 32.145	0.0	0.0	0.0	0.0	0.0	0.0
31.145 / 32.15	0.0	0.0	0.0	0.0	0.0	0.0
31.15 / 32.155	0.0	0.0	0.0	0.0	0.0	0.0
31.155 / 32.16	0.0	0.0	0.0	0.0	0.0	0.0
31.16 / 32.165	0.2	0.2	0.2	0.2	0.2	0.2
31.165 / 32.17	0.4	0.6	0.6	0.6	0.6	0.4
31.17 / 32.175	0.8	0.8	0.8	0.8	1.6	0.8
31.175 / 32.18	1.0	1.0	0.8	1.0	1.6	0.8
31.18 / 32.185	1.0	1.2	1.2	1.2	1.8	1.0
31.185 / 32.19	1.4	1.2	1.2	1.4	1.8	1.2
31.19 / 32.195	1.4	1.4	1.6	1.6	2.2	1.4
31.195 / 32.2	1.2	1.4	1.4	1.4	1.4	1.2
31.2 / 32.205	1.2	1.2	1.4	1.6	2.0	1.2
31.205 / 32.21	1.4	1.2	1.4	1.8	2.2	1.2
31.21 / 32.215	1.4	1.4	1.6	1.8	2.0	1.4
31.215 / 32.22	1.2	1.2	1.4	1.6	1.8	1.2
31.22 / 32.225	1.4	1.6	1.8	2.0	2.6	1.4
31.225 / 32.23	1.6	1.4	1.8	2.2	3.0	1.4
31.23 / 32.235	1.6	1.4	1.6	2.2	2.8	1.4
31.235 / 32.24	1.6	1.8	1.8	2.4	2.6	1.6
31.24 / 32.245	2.0	2.2	1.8	1.6	1.8	1.6
31.245 / 32.25	0.6	0.6	0.6	1.0	1.0	0.6
31.25 / 32.255	0.6	0.8	0.8	1.2	1.4	0.6
31.255 / 32.26	0.8	0.8	0.8	1.2	1.2	0.8
31.26 / 32.265	1.0	1.2	1.4	1.6	2.2	1.0
31.265 / 32.27	0.8	0.8	1.2	1.8	2.4	0.8
31.27 / 32.275	0.4	0.8	0.8	1.4	2.6	0.4
31.275 / 32.28	1.0	1.2	1.4	2.0	2.6	1.0
31.28 / 32.285	1.8	1.8	2.0	2.2	2.4	1.8
31.285 / 32.29	1.8	1.8	2.4	2.4	2.8	1.8
31.29 / 32.295	2.2	2.2	2.4	2.6	3.2	2.2
31.295 / 32.3	2.4	2.6	2.8	3.0	3.4	2.4
31.3 / 32.305	2.4	2.6	2.6	3.2	3.4	2.4
31.305 / 32.31	2.6	2.8	2.6	2.8	2.8	2.6
31.31 / 32.315	2.4	2.6	2.2	2.4	2.6	2.2
31.315 / 32.32	2.2	1.4	1.6	1.6	1.8	1.4
31.32 / 32.325	1.6	1.2	1.0	1.0	1.0	1.0
31.325 / 32.33	0.0	0.0	0.0	0.0	0.0	0.0

Table 6: Calcaulated DA in the tune scan of Yellow ring with $\beta^* = 0.6$ m lattices. dp/p0=0.0017 and with re-bucketing.

	Workign points	Dynamic aperture [unit: σ]					
		15°	30°	45°	60°	75°	Minimum
Yellow ring:							
	31.1 / 32.105	2.8	3.0	2.8	2.8	3.2	2.8
	31.105 / 32.11	3.0	3.2	3.4	3.6	3.6	3.0
	31.11 / 32.115	3.6	3.6	3.4	3.8	3.8	3.4
	31.115 / 32.12	3.0	3.2	3.2	3.4	3.6	3.0
	31.12 / 32.125	3.2	3.4	3.2	3.6	3.4	3.2
	31.125 / 32.13	3.4	3.0	3.4	3.6	3.6	3.0
	31.13 / 32.135	3.0	3.6	3.0	3.2	3.4	3.0
	31.135 / 32.14	2.6	2.6	2.6	2.8	2.6	2.6
	31.14 / 32.145	2.8	3.0	2.8	3.2	2.6	2.6
	31.145 / 32.15	3.4	3.2	3.6	3.4	3.4	3.2
	31.15 / 32.155	3.6	4.0	3.4	3.4	4.0	3.4
	31.155 / 32.16	2.8	2.4	2.8	2.8	2.4	2.4
	31.16 / 32.165	2.0	2.2	2.2	2.2	2.0	2.0
	31.165 / 32.17	2.4	2.2	2.2	2.4	2.0	2.0
	31.17 / 32.175	4.0	4.0	4.0	4.0	4.0	4.0
	31.175 / 32.18	4.3	4.1	4.3	4.3	4.5	4.1
	31.18 / 32.185	2.2	2.0	2.4	2.0	2.0	2.0
	31.185 / 32.19	1.8	1.6	1.6	2.0	1.4	1.4
	31.19 / 32.195	2.0	2.0	2.0	1.8	2.0	1.8
	31.195 / 32.2	2.0	1.8	1.6	1.6	1.8	1.6
	31.2 / 32.205	3.0	3.0	3.2	3.4	3.6	3.0
	31.205 / 32.21	4.3	4.5	4.3	4.3	4.3	4.3
	31.21 / 32.215	4.5	4.5	4.7	4.5	4.5	4.5
	31.215 / 32.22	4.3	4.1	4.3	4.3	4.7	4.1
	31.22 / 32.225	2.6	2.8	2.4	2.8	2.4	2.4
	31.225 / 32.23	1.8	1.8	1.8	1.6	1.8	1.6
	31.23 / 32.235	1.6	1.6	1.4	1.4	1.2	1.2
	31.235 / 32.24	1.6	1.4	1.4	1.4	1.4	1.4
	31.24 / 32.245	1.2	1.2	1.2	1.2	1.0	1.0
	31.245 / 32.25	0.6	0.8	1.0	1.0	1.6	0.6
	31.25 / 32.255	2.0	2.2	2.0	1.8	2.0	1.8
	31.255 / 32.26	4.0	3.8	4.3	4.0	4.1	3.8
	31.26 / 32.265	3.8	3.8	3.8	3.6	3.8	3.6
	31.265 / 32.27	3.0	3.0	3.2	3.0	3.2	3.0
	31.27 / 32.275	3.0	3.0	2.8	3.0	3.0	2.8
	31.275 / 32.28	3.0	3.0	2.8	2.8	2.8	2.8
	31.28 / 32.285	3.0	3.2	3.2	3.2	3.2	3.0
	31.285 / 32.29	1.2	1.0	1.4	1.6	2.2	1.0
	31.29 / 32.295	1.2	1.0	0.8	0.8	1.6	0.8
	31.295 / 32.3	0.8	0.6	0.8	0.8	0.6	0.6
	31.3 / 32.305	0.0	0.0	0.0	0.0	0.0	0.0
	31.305 / 32.31	0.0	0.0	0.0	0.0	0.0	0.0
	31.31 / 32.315	0.0	0.0	0.0	0.0	0.0	0.0
	31.315 / 32.32	0.0	0.0	0.0	0.0	0.0	0.0
	31.32 / 32.325	0.2	0.2	0.2	0.0	0.0	0.0
	31.325 / 32.33	0.0	0.0	0.0	0.0	0.0	0.0

Table 7: Calculated dynamic aperture in the tune scan with $\beta^* = 0.7$ m lattices. dp/p0=0.0017 and with re-bucketing. With IR nonlinearities. Without Q" correction.

	Workign points	Dynamic aperture [unit: σ]					
		15°	30°	45°	60°	75°	Minimum
Blue ring:							
	31.2 / 32.2025	1.6	1.4	1.4	1.4	1.6	1.4
	31.2025 / 32.205	1.8	1.4	1.4	1.8	1.6	1.4
	31.205 / 32.2075	1.8	1.6	1.6	1.8	1.8	1.6
	31.2075 / 32.21	1.6	1.4	1.6	1.6	1.8	1.4
	31.21 / 32.2125	1.8	1.4	1.6	1.6	1.8	1.4
	31.2125 / 32.215	2.0	1.6	2.0	2.0	2.2	1.6
	31.215 / 32.2175	1.8	1.8	2.0	2.0	2.2	1.8
	31.2175 / 32.22	2.0	1.8	2.0	1.8	2.0	1.8
	31.22 / 32.2225	1.6	1.4	1.6	1.8	2.2	1.4
	31.2225 / 32.225	1.4	1.8	2.2	2.2	2.2	1.4
	31.225 / 32.2275	1.8	2.0	2.2	2.2	2.4	1.8
	31.2275 / 32.23	2.4	2.2	2.4	2.6	2.6	2.2
	31.23 / 32.2325	2.4	2.2	2.8	2.6	3.2	2.2
	31.2325 / 32.235	2.6	2.4	2.6	2.6	2.8	2.4
	31.235 / 32.2375	2.8	2.2	2.2	2.6	2.6	2.2
	31.2375 / 32.24	2.6	2.2	2.6	2.6	2.8	2.2
	31.24 / 32.2425	2.8	2.0	2.0	2.4	2.2	2.0
	31.2425 / 32.245	1.4	1.6	1.6	1.4	1.4	1.4
	31.245 / 32.2475	1.8	0.4	0.4	0.6	0.8	0.4
	31.2475 / 32.25	1.0	1.0	1.2	1.4	1.4	1.0
Yellow ring:							
	31.2 / 32.2025	3.8	3.6	3.4	4.0	4.0	3.4
	31.2025 / 32.205	4.7	4.1	4.7	4.7	4.5	4.1
	31.205 / 32.2075	4.9	5.1	5.1	5.1	5.3	4.9
	31.2075 / 32.21	5.3	5.1	5.1	5.5	5.3	5.1
	31.21 / 32.2125	5.1	4.9	4.9	5.1	5.3	4.9
	31.2125 / 32.215	4.5	4.9	4.5	4.9	5.1	4.5
	31.215 / 32.2175	3.8	4.7	4.1	4.5	4.5	3.8
	31.2175 / 32.22	4.7	4.1	4.5	4.7	4.5	4.1
	31.22 / 32.2225	4.5	4.9	4.9	5.1	4.9	4.5
	31.2225 / 32.225	4.5	4.7	4.1	4.5	4.7	4.1
	31.225 / 32.2275	3.0	3.2	3.4	3.6	3.6	3.0
	31.2275 / 32.23	1.8	2.0	2.4	2.2	2.4	1.8
	31.23 / 32.2325	1.8	1.8	1.6	1.8	2.0	1.6
	31.2325 / 32.235	1.8	2.0	1.6	1.4	1.8	1.4
	31.235 / 32.2375	2.0	2.0	1.8	1.6	1.8	1.6
	31.2375 / 32.24	2.0	1.8	1.8	1.4	1.2	1.2
	31.24 / 32.2425	1.4	1.6	1.2	1.2	1.2	1.2
	31.2425 / 32.245	1.2	1.2	1.2	1.2	1.2	1.2
	31.245 / 32.2475	1.6	1.6	1.4	1.4	1.4	1.4
	31.2475 / 32.25	2.2	1.8	1.8	1.6	1.6	1.6

Table 8: Calculated dynamic aperture in the tune scan with $\beta^* = 0.7$ m lattices. dp/p0=0.0017 and with re-bucketing. Without IR nonlinearities and Q" correction.

	Workign points	Dynamic aperture [unit: σ]					
		15°	30°	45°	60°	75°	Minimum
Blue ring:							
	31.2 / 32.2025	6.3	4.1	5.7	6.3	8.3	4.1
	31.2025 / 32.205	6.7	4.3	5.1	6.3	8.1	4.3
	31.205 / 32.2075	6.7	5.3	5.5	6.7	8.4	5.3
	31.2075 / 32.21	6.1	4.5	5.7	7.9	11.0	4.5
	31.21 / 32.2125	6.3	5.7	5.9	6.9	10.0	5.7
	31.2125 / 32.215	4.0	5.7	5.9	8.3	11.0	4.0
	31.215 / 32.2175	4.9	5.7	4.5	9.4	11.4	4.5
	31.2175 / 32.22	6.3	5.9	6.1	9.6	12.7	5.9
	31.22 / 32.2225	7.1	6.3	6.3	8.3	12.7	6.3
	31.2225 / 32.225	7.9	7.3	7.7	8.4	12.9	7.3
	31.225 / 32.2275	8.1	8.1	8.4	9.2	12.5	8.1
	31.2275 / 32.23	8.4	8.6	8.8	12.5	12.7	8.4
	31.23 / 32.2325	8.6	8.6	9.0	12.5	12.2	8.6
	31.2325 / 32.235	8.8	8.8	9.0	12.5	10.8	8.8
	31.235 / 32.2375	8.8	8.8	9.0	10.2	9.0	8.8
	31.2375 / 32.24	8.8	8.3	8.3	7.9	7.1	7.1
	31.24 / 32.2425	6.7	6.1	6.3	5.7	5.7	5.7
	31.2425 / 32.245	6.1	4.7	5.1	3.4	4.1	3.4
	31.245 / 32.2475	4.0	4.0	3.4	3.2	3.4	3.2
	31.2475 / 32.25	3.8	1.6	3.8	1.8	2.2	1.6
Yellow ring:							
	31.2 / 32.2025	11.8	11.6	9.2	9.6	15.7	9.2
	31.2025 / 32.205	15.1	13.3	12.7	14.1	15.5	12.7
	31.205 / 32.2075	16.1	15.1	15.7	15.7	15.7	15.1
	31.2075 / 32.21	16.3	16.6	16.3	15.9	15.7	15.7
	31.21 / 32.2125	16.3	15.7	14.9	16.1	15.7	14.9
	31.2125 / 32.215	16.5	15.7	15.7	15.5	15.9	15.5
	31.215 / 32.2175	15.5	16.6	16.3	16.5	15.7	15.5
	31.2175 / 32.22	15.1	16.1	15.1	16.5	15.9	15.1
	31.22 / 32.2225	12.5	12.2	14.1	13.1	14.7	12.2
	31.2225 / 32.225	9.2	8.8	10.0	10.2	13.3	8.8
	31.225 / 32.2275	8.6	7.7	7.7	9.4	11.2	7.7
	31.2275 / 32.23	6.3	6.7	8.3	7.9	8.8	6.3
	31.23 / 32.2325	7.1	5.5	6.7	6.7	6.9	5.5
	31.2325 / 32.235	5.9	5.5	4.5	5.5	5.3	4.5
	31.235 / 32.2375	5.5	5.9	5.7	4.9	4.3	4.3
	31.2375 / 32.24	5.3	5.1	4.1	5.5	6.1	4.1
	31.24 / 32.2425	6.1	5.9	4.9	4.9	4.9	4.9
	31.2425 / 32.245	4.7	4.3	3.8	3.4	2.8	2.8
	31.245 / 32.2475	5.5	5.5	4.5	5.1	5.5	4.5
	31.2475 / 32.25	6.5	5.7	6.7	5.5	9.6	5.5

Table 9: Calculated dynamic aperture in the tune scan with $\beta^* = 0.7$ m lattices. dp/p0=0.0017 and with re-bucketing. With Q" correction.

	Workign points	Dynamic aperture [unit: σ]					
		15°	30°	45°	60°	75°	Minimum
Blue ring:							
	31.2 / 32.2025	2.0	2.0	2.4	2.2	2.8	2.0
	31.2025 / 32.205	2.2	3.0	2.6	3.0	3.2	2.2
	31.205 / 32.2075	3.0	3.0	3.2	3.6	4.0	3.0
	31.2075 / 32.21	3.6	3.4	3.4	4.0	4.0	3.4
	31.21 / 32.2125	4.0	3.8	3.8	4.1	4.3	3.8
	31.2125 / 32.215	4.3	4.1	4.1	4.1	4.3	4.1
	31.215 / 32.2175	4.3	4.3	4.3	4.1	4.0	4.0
	31.2175 / 32.22	4.5	4.5	4.1	3.8	4.1	3.8
	31.22 / 32.2225	4.1	4.5	4.1	4.0	4.1	4.0
	31.2225 / 32.225	4.0	4.0	4.0	4.1	4.3	4.0
	31.225 / 32.2275	4.0	4.0	4.0	4.3	4.3	4.0
	31.2275 / 32.23	4.1	4.3	4.3	4.1	4.3	4.1
	31.23 / 32.2325	4.3	4.1	4.3	4.1	4.1	4.1
	31.2325 / 32.235	4.0	4.0	4.1	3.8	4.0	3.8
	31.235 / 32.2375	3.8	3.8	3.6	3.6	3.4	3.4
	31.2375 / 32.24	3.4	3.2	3.2	2.8	3.0	2.8
	31.24 / 32.2425	2.2	2.2	2.2	2.2	2.0	2.0
	31.2425 / 32.245	1.8	1.8	1.6	1.2	1.2	1.2
	31.245 / 32.2475	2.0	2.0	1.6	1.2	1.0	1.0
	31.2475 / 32.25	1.6	1.4	0.8	1.0	1.0	0.8
Yellow ring:							
	31.2 / 32.2025	2.4	2.6	2.6	2.6	3.0	2.4
	31.2025 / 32.205	3.0	3.4	3.4	3.4	3.8	3.0
	31.205 / 32.2075	4.0	4.1	4.7	4.7	4.7	4.0
	31.2075 / 32.21	4.9	5.1	4.9	4.9	5.7	4.9
	31.21 / 32.2125	4.7	4.7	5.1	5.1	5.3	4.7
	31.2125 / 32.215	4.5	4.7	4.5	4.7	4.9	4.5
	31.215 / 32.2175	4.3	4.3	4.5	4.3	4.7	4.3
	31.2175 / 32.22	4.0	4.3	4.5	4.3	4.5	4.0
	31.22 / 32.2225	4.5	4.3	4.1	4.7	4.9	4.1
	31.2225 / 32.225	4.9	4.5	4.9	5.1	5.1	4.5
	31.225 / 32.2275	4.7	4.7	4.7	4.7	4.9	4.7
	31.2275 / 32.23	3.6	3.4	3.8	3.8	3.8	3.4
	31.23 / 32.2325	2.8	3.0	2.8	3.0	3.2	2.8
	31.2325 / 32.235	2.2	2.2	2.2	2.4	2.4	2.2
	31.235 / 32.2375	1.6	2.2	2.2	2.4	2.4	1.6
	31.2375 / 32.24	2.0	2.0	2.2	2.2	2.2	2.0
	31.24 / 32.2425	1.2	1.2	1.2	1.2	1.2	1.2
	31.2425 / 32.245	1.4	1.6	1.6	1.6	1.6	1.4
	31.245 / 32.2475	0.0	0.0	0.0	1.0	1.2	0.0
	31.2475 / 32.25	1.4	1.4	1.4	1.8	2.0	1.4